Electrical Power and Energy Systems 118 (2020) 105762

Contents lists available at ScienceDirect

Electrical Power and Energy Systems

journal homepage: www.elsevier.com/locate/ijepes

Risk-based dynamic generation and transmission expansion planning with propagating effects of contingencies

Mahdi Mehrtash, Amin Kargarian*

Electrical and Computer Engineering Department, Louisiana State University, Baton Rouge, LA 70803, USA

ARTICLE INFO

Keywords:
Generation and transmission expansion planning
McCormick relaxation
$N-1$ security criteria
Risk index
Second-order cone programming

ABSTRACT

Transmission networks and generating units must be reinforced to satisfy the ever-increasing demand for electricity and to keep power system reliability within an acceptable level. According to the standards, the planned power system must be able to supply demand in the case of outage of a single element ($\boldsymbol{N}-1$ security criteria), and the possibility of cascading failures must be minimized. In this paper, we propose a risk-based dynamic generation and transmission expansion planning model with respect to the propagating effect of each contingency on the power system. Using the concept of risk, post-contingency load-shedding penalty costs are obtained and added in the objective function to penalize high-risk contingencies more dominantly. The McCormick relaxation is tailored to alter the objective function into a linear format. To keep the practicality of the proposed model, a second-order cone programming model is applied for power flow representation, and the problem is modeled in a dynamic time frame. The proposed model is formulated as a mixed-integer second-order cone programming problem. The numerical studies on the RTS 24-bus test system illustrate the efficacy of the proposed model.

1. Introduction

1.1. Background and motivation

Power system expansion planning is necessary to satisfy load growth and to keep system reliability within an acceptable level. Transmission networks and generating units should be reinforced with new lines and units in certain planning horizons [1]. Since transmission expansion planning (TEP) and generation expansion planning (GEP) problems are interrelated, it is more advantageous to have a solution that is optimal for both problems. A joint generation and transmission expansion planning (G&TEP) problem determines a generation and transmission expansion plan that is most beneficial for the system as a whole [2].

A G&TEP model is tackled either in a market-based framework or a centralized framework. In the market-based framework, profit-oriented agents determine their own G&TEP plans with the aim of maximizing their expected profits. On the other hand, in the centralized approach, a central planner, e.g., the independent system operator (ISO), determines the G&TEP plan that has the highest profit for the whole system. Then, the central planner encourages private entities, by incentives, to expand their system accordingly [2]. In this paper, we deal with the centralized approach for the G&TEP problem.

Similar to the TEP and GEP, G&TEP decisions can be made either at a single point in time (static model) or at different points in time (dynamic model). As suggested in the literature, the dynamic G&TEP model is superior in comparison to the static one. In the static model, demand at the end of the planning horizon is considered. Since the G&TEP is a long-term planning problem, demand at the end of the planning horizon is higher than that at the beginning of the horizon or in the short-term. Thus, the decisions made by the static model result in an overcapacity that is not needed until the end of the planning horizon. While using the dynamic approach, the capacity can be added to the system as needed, and it allows us to adjust to possible changes in system conditions throughout the planning horizon [3]. However, the size of the G&TEP problem has a direct impact on computational complexity. Therefore, the size of the problem should be taken into account for selecting the G&TEP model and the solution algorithm. In this paper, we consider the dynamic approach for G&TEP.

Power system contingencies (e.g., outage of transmission lines and generating units) might have catastrophic results on the system and society. According to the North American Electric Reliability Corporation, Standard 51 [4], a planned network must be able to supply demands in the case of outage of a single element ($N-1$ security criteria). Therefore, considering $N-1$ security criteria for G&TEP is essential. The best way to model $N-1$ security criteria in G&TEP is, however, still an ongoing research topic.

* Corresponding author.
E-mail addresses: mmehrt3@lsu.edu (M. Mehrtash), kargarian@lsu.edu (A. Kargarian).

https://doi.org/10.1016/j.ijepes.2019.105762
Received 12 August 2019; Received in revised form 31 October 2019; Accepted 5 December 2019

1.2. Literature review

A systematic approach to determine the most significant contingencies for an $N-1$ security-constrained TEP problem is presented in [5]. However, this model is not tractable for stochastic TEP due to the accumulative effect of considering all scenarios at the beginning of the decision-making process. Thus, new identification indices are proposed by [6] to integrate the necessary contingencies gradually for each iteration of the stochastic TEP model. A TEP model with probabilistic reliability criteria is presented in [7]. The suitability of the model subject to future uncertainties is demonstrated. A mixed-integer linear programming (MILP) model for G&TEP is presented in [8]. Probabilistic reliability criteria for random generator and line outages with known historical outage rates are considered. Although these references (and many other papers) assume that all possible contingencies have identical consequences on the rest of the system, the probability and consequence of contingencies are not the same in practice. Because of specific characteristics (e.g., topology) of power systems, some contingencies might lead to other outages, and extremely, cascading failure of the system [9,10]. Therefore, it is oversimplified to consider identical consequences for different contingencies. As will be shown later, ignoring this concept may degrade the quality and effectiveness of planning results.

A conic relaxation is proposed in [11] for power flow modeling of a network expansion planning problem. The obtained solutions satisfy the stipulated AC power flow constraints. Furthermore, a bi-level optimization model for TEP considering second-order cone programming (SOCP) is developed in [12]. Instead of the linearized DC model, a convexification technique is used to model the flow of existing and candidate transmission lines. In this paper, a SOCP model, which is more accurate and practical than linearized DC models, is tailored for network power flow representation.

1.3. Contributions

In this paper, we propose a risk-based dynamic G&TEP model taking into account the propagating effects of contingencies on the rest of the system. Two performance indices, i.e., MW performance index and voltage-reactive power performance index, are developed to model the effect of each contingency on the rest of the system. Then, using the concept of risk, non-identical post-contingency load-shedding penalty costs are determined for different contingencies. The penalty cost of each contingency is added to the objective function of the dynamic G&TEP model. That is, high-risk contingencies are penalized more dominantly. As a result, expenses for maintaining system reliability during an expansion planning will be spent more wisely. Appending the developed risk index in the objective function makes the problem nonlinear. The McCormick relaxation is tailored to alter the objective function into a linear format. To keep the practicality of the proposed model, a SOCP model is applied for power flow representation of the network, and the problem is modeled in a dynamic time frame. The proposed model can be solved by a standard solver, e.g., CPLEX, as a mixed-integer second-order cone programming (MISOCP) problem.

1.4. Paper structure

The remainder of the paper is organized as follows. The conventional dynamic G&TEP problems with and without considering $N-1$ security criteria are presented in Section 2. The proposed risk-based dynamic G&TEP model and the McCormick relaxation technique are deliberated in Section 3. Numerical results are discussed in Section 4. Concluding remarks are provided in Section 5.

2. Dynamic G&TEP problem formulation

A nomenclature for the presented formulation is given in the Appendix.

2.1. Conventional dynamic G&TEP

Ignoring $N-1$ security criteria, the objective function of the dynamic G&TEP problem is modeled by (1), where the set of decision variables is given by (2). The objective function includes the cost of installing new generating units and transmission lines (investment costs) plus the cost of generation and load shedding (operation costs) for all considered operating conditions o.

$$\min_{\Delta} \sum_{\forall t} \Big\{ a_{lt} \sum_{l\in\Omega^{L+}} \widetilde{I}_l . x_{lt} + a_{gt} \sum_{g\in\Omega^{G+}} \widetilde{I}_g . x_{gt} + \sum_{\forall o} \rho_o [\sum_{\forall g} C_g . P_{got} + \sum_{\forall d} C_{do} \cdot \Gamma_{dot}] \Big\} \tag{1}$$

$$\Delta = \{x_{lt}, x_{gt}, P_{got}, Q_{got}, \Gamma_{dot}, P_{lot}, Q_{lot}, u_{not}, R_{not}, L_{not}\} \tag{2}$$

Constraints (3) and (4) model the budget limitation of the planning entity for each planning period t. Constraints (5) and (6) are necessary to ensure that a prospective transmission line or generating unit will be installed only once during the whole planning horizon. Nodal active and reactive power balance constraints are given in (7) and (8), respectively. Γ_{dot} is the expected energy not supplied for demand d in operating condition o at time period t during normal operation.

$$\sum_{l\in\Omega^{L+}} \widetilde{I}_l \cdot x_{lt} \le \widetilde{I}_{lt}^{max}; \forall\ t \tag{3}$$

$$\sum_{g\in\Omega^{G+}} \widetilde{I}_g \cdot x_{gt} \le \widetilde{I}_{gt}^{max}; \forall\ t \tag{4}$$

$$\sum_{\forall t} x_{lt} \le 1; \forall\ l \in \Omega^{L+} \tag{5}$$

$$\sum_{\forall t} x_{gt} \le 1; \forall\ g \in \Omega^{G+} \tag{6}$$

$$\sum_{\forall g\in\Omega_n^{G,G^+}} P_{got} - \sum_{\forall l|s(l)=n} P_{lot} + \sum_{\forall l|r(l)=n} P_{lot} = \sum_{d\in\Omega_n^D} (P_{dot} - \Gamma_{dot}); \forall\ n, o, t \tag{7}$$

$$\sum_{\forall g\in\Omega_n^{G,G^+}} Q_{got} - \sum_{\forall l|s(l)=n} Q_{lot} + \sum_{\forall l|r(l)=n} Q_{lot} = \sum_{d\in\Omega_n^D} (Q_{dot} - \alpha_d \cdot \Gamma_{dot}); \forall\ n, o, t \tag{8}$$

Instead of the linear DC power flow, a SOCP, which is a convex version of the full AC representation, is applied to make the model more realistic. The transmission system is assumed to be balanced. Given the second-order cone model, active and reactive powers flow through each existing transmission line can be obtained by (9) and (10), respectively. R_{lot} and L_{lot} are auxiliary variables to construct the convex AC power flow, and u_{not} is the voltage magnitude in the conic model. Capacity limitation of existing transmission lines is modeled in (11) and (12). Similarly, active and reactive powers flowing through each candidate transmission line is formulated by (13) and (14), respectively. P_{lot} and Q_{lot} are nonzero if the candidate transmission line is planned to be built at the beginning of the planning period t or it was built in previous periods (i.e., $\sum_{\forall \tau \le t} x_{l\tau} = 1$). Having the nonlinear constraints (13) and (14) in the model leads to a mixed-integer nonlinear programming (MINLP) problem, which is not desired. Therefore, to model the power flow of candidate transmission lines, (13) and (14) are linearized as (15)-(18) using a disjunctive technique [13].

$$P_{lot} = \sqrt{2} G_l u_{not} - G_l R_{lot} + B_l L_{lot}; \forall\ l \in \Omega^L, o, t, n = s(l) \tag{9}$$

$$Q_{lot} = \sqrt{2} (B_l + B_l^{sh}/2) u_{not} - B_l R_{lot} - G_l L_{lot}; \forall\ l \in \Omega^L, o, t, n = s(l) \tag{10}$$

$$-P_l^{max} \le P_{lot} \le P_l^{max};\quad \forall\, l \in \Omega^L,\ o,\ t \tag{11}$$

$$-Q_l^{max} \le Q_{lot} \le Q_l^{max};\quad \forall\, l \in \Omega^L,\ o,\ t \tag{12}$$

$$P_{lot} = (\sqrt{2}G_l u_{not} - G_l R_{lot} + B_l L_{lot})\cdot \sum_{\forall \tau \le t} x_{l\tau};\ \forall\, l \in \Omega^{L+},\ o,\ t,\ n = s(l) \tag{13}$$

$$Q_{lot} = \left(\sqrt{2}\left(B_l + \frac{B_l^{sh}}{2}\right)u_{not} - B_l R_{lot} - G_l L_{lot}\right)\cdot \sum_{\forall \tau \le t} x_{l\tau};\ \forall\, l \in \Omega^{L+},\ o,\ t,\ n = s(l) \tag{14}$$

$$-\left(1 - \sum_{\forall \tau \le t} x_{l\tau}\right)\cdot M \le P_{lot} - \{\sqrt{2}G_l u_{not} - G_l R_{lot} + B_l L_{lot}\} \le \left(1 - \sum_{\forall \tau \le t} x_{l\tau}\right)\cdot M;\ \forall\, l \in \Omega^{L+},\ o,\ t,\ n = s(l) \tag{15}$$

$$-\left(1 - \sum_{\forall \tau \le t} x_{l\tau}\right)\cdot M \le Q_{lot} - \{\sqrt{2}(B_l + B_l^{sh}/2)u_{not} - B_l R_{lot} - G_l L_{lot}\} \le \left(1 - \sum_{\forall \tau \le t} x_{l\tau}\right)\cdot M;\ \forall\, l \in \Omega^{L+},\ o,\ t,\ n = s(l) \tag{16}$$

$$-P_l^{max}\cdot \sum_{\forall \tau \le t} x_{l\tau} \le P_{lot} \le P_l^{max}\cdot \sum_{\forall \tau \le t} x_{l\tau};\ \forall\, l \in \Omega^{L+},\ o,\ t \tag{17}$$

$$-Q_l^{max}\cdot \sum_{\forall \tau \le t} x_{l\tau} \le Q_{lot} \le Q_l^{max}\cdot \sum_{\forall \tau \le t} x_{l\tau};\ \forall\, l \in \Omega^{L+},\ o,\ t \tag{18}$$

The active power generation limit of the existing and candidate units is imposed by (19) and (20), respectively. Likewise, (21)-(22) restrict the reactive power generation limits. Eq. (23) guarantees that the expected energy not supplied cannot be larger than the corresponding demand. Binary decision variables for each planning period are defined in (24). The thermal capacity limit of transmission lines is modeled by (25). The conic constraint is presented by (26), and constraints of the auxiliary variables are shown in (27) and (28). The permissible voltage magnitude of each node is imposed by (29). The association between conic variables (u_{not}, R_{lot}, and L_{lot}) and magnitude/angle of the nodal voltages ($V_{not}/\theta_{\{nm\}ot}$) is shown in (30)–(32). They can be used to calculate the nodal voltage magnitudes and voltage angles after obtaining the solution of MISOCP. Eq. (33) fixes the voltage magnitude of the reference node to one.

Power losses can also be considered in the G&TEP model. Losses can be incorporated in the objective function as a penalty term or can be limited by introducing new constraints. The way that losses are modeled depends on the planner's preference. If losses are modeled as a new set of constraints, the problem would be tighter. If losses are incorporated in the objective function as a penalty term, the solution depends on the penalty coefficient. Either of these modelings may result in installing more new lines.

$$0 \le P_{got} \le P_g^{max};\quad \forall\, g \in \Omega^G,\ o,\ t \tag{19}$$

$$0 \le P_{got} \le P_g^{max}\cdot \sum_{\forall \tau \le t} x_{g\tau};\quad \forall\, g \in \Omega^{G+},\ o,\ t \tag{20}$$

$$0 \le Q_{got} \le Q_g^{max};\quad \forall\, g \in \Omega^G,\ o,\ t \tag{21}$$

$$0 \le Q_{got} \le Q_g^{max}\cdot \sum_{\forall \tau \le t} x_{g\tau};\quad \forall\, g \in \Omega^{G+},\ o,\ t \tag{22}$$

$$0 \le \Gamma_{dot} \le P_{dot};\quad \forall\, d,\ o,\ t \tag{23}$$

$$x_{gt},\ x_{lt} \in \{0, 1\};\quad \forall\, g \in \Omega^{G+},\ l \in \Omega^{L+},\ t \tag{24}$$

$$(P_{lot})^2 + (Q_{lot})^2 \le (S_l^{max})^2;\quad \forall\, l \in \{\Omega^{L+}, \Omega^L\},\ o,\ t \tag{25}$$

$$2u_{not}u_{mot} \ge (R_{lot})^2 + (L_{lot})^2;\quad \forall\, l \in \{\Omega^{L+}, \Omega^L\},\ o,\ t,\ n = s(l),\ m = r(l) \tag{26}$$

$$R_{\{nm\}ot} = R_{\{mn\}ot} \ge 0;\quad \forall\, l \in \{\Omega^{L+}, \Omega^L\},\ o,\ t,\ n = s(l),\ m = r(l) \tag{27}$$

$$L_{\{nm\}ot} = -L_{\{mn\}ot};\quad \forall\, l \in \{\Omega^{L+}, \Omega^L\},\ o,\ t,\ n = s(l),\ m = r(l) \tag{28}$$

$$\frac{(V_n^{min})^2}{\sqrt{2}} \le u_{not} \le \frac{(V_n^{max})^2}{\sqrt{2}};\quad \forall\, n,\ o,\ t \tag{29}$$

$$u_{not} = \frac{V_{not}^2}{\sqrt{2}};\quad \forall\, n,\ o,\ t \tag{30}$$

$$R_{lot} = V_{not}V_{mot}\cos\theta_{\{nm\}ot};\ \forall\, l \in \{\Omega^{L+}, \Omega^L\},\ o,\ t,\ n = s(l),\ m = r(l) \tag{31}$$

$$L_{lot} = V_{not}V_{mot}\sin\theta_{\{nm\}ot};\ \forall\, l \in \{\Omega^{L+}, \Omega^L\},\ o,\ t,\ n = s(l),\ m = r(l) \tag{32}$$

$$u_{not} = \frac{1}{\sqrt{2}};\quad \forall\, n = ref,\ o,\ t \tag{33}$$

Finally, the conventional dynamic G&TEP problem is expressed as minimizing (1) subject to (3)–(12), (15)–(29), and (33).

2.2. Security-constrained dynamic G&TEP

$N-1$ security constraints must be considered in G&TEP to ensure system security. For this purpose, penalty terms representing load-shedding after contingency should be appended to the objective function as presented in (34). Note that the value of load-shedding penalty cost after contingency (C_{dot}^c) is different than the cost of load-shedding in normal operation (C_{dot}). In addition to the set of decision variables in normal operation, (2), a new set of decision variables appears in (35) is required to build the security-constrained G&TEP model.

$$\min_{\Delta,\Delta^c} \sum_{\forall t} \Big\{ a_{lt} \sum_{l \in \Omega^{L+}} \widetilde{I}_l\cdot x_{lt} + a_{gt} \sum_{g \in \Omega^{G+}} \widetilde{I}_g\cdot x_{gt} + \sum_{\forall o} \rho_o \Big[\sum_{\forall g} C_g\cdot P_{got} + \sum_{\forall d} C_{dot}\cdot \Gamma_{dot} + \sum_{\forall c \in \{\Omega_c^L, \Omega_c^{L+}\}} \sum_{\forall d} \Big(C_{dot}^c\cdot \sum_{\forall \tau \le t} x_{l\tau}\cdot \Gamma_{dot}^c\Big) + \sum_{\forall c \in \{\Omega_c^G, \Omega_c^{G+}\}} \sum_{\forall d} \Big(C_{dot}^c\cdot \sum_{\forall \tau \le t} x_{g\tau}\cdot \Gamma_{dot}^c\Big)\Big]\Big\} \tag{34}$$

$$\Delta^c = \{P_{got}^c,\ Q_{got}^c,\ \Gamma_{dot}^c,\ P_{lot}^c,\ Q_{lot}^c,\ u_{not}^c,\ R_{not}^c,\ L_{not}^c\} \tag{35}$$

Active and reactive nodal power balance constraints for contingency c are modeled by (36) and (37). The power flow constraints of existing lines during contingency c are formulated as (38)–(41), where A_l^c is a parameter that is equal to 0 if line l is unavailable under contingency c, and 1 otherwise. Furthermore, the linearized power flow constraints of candidate transmission lines during contingency c are modeled in (42)–(45). Eqs. (46)–(49) represent active and reactive power generation limits of the existing and candidate units during contingency c, where A_g^c is a parameter that is equal to 0 if unit g is unavailable under contingency c, and 1 otherwise. Having normal operation constraints of (23)–(33), similar constraints need to be imposed for each contingency c (i.e., (23)–(33); $\forall\, c$). The adjustment capability limit of generating units during a contingency is modeled by (50). For specific values of $\Delta_g^{max} \ne 0/\Delta_g^{max} = 0$, generating unit g has a corrective/preventive role in case of contingency.

$$\sum_{\forall g \in \Omega_n^{G,G^+}} P_{got}^c - \sum_{\forall l | s(l)=n} P_{lot}^c + \sum_{\forall l | r(l)=n} P_{lot}^c = \sum_{d \in \Omega_n^D} (P_{dot} - \Gamma_{dot}^c);\ \forall\, n,\ o,\ t,\ c \tag{36}$$

$$\sum_{\forall g \in \Omega_n^{G,G^+}} Q_{got}^c - \sum_{\forall l | s(l)=n} Q_{lot}^c + \sum_{\forall l | r(l)=n} Q_{lot}^c = \sum_{d \in \Omega_n^D} (Q_{dot} - \alpha_d\cdot \Gamma_{dot}^c);\ \forall\, n,\ o,\ t,\ c \tag{37}$$

$$P_{lot}^c = A_l^c\cdot(\sqrt{2}G_l u_{not}^c - G_l R_{lot}^c + B_l L_{lot}^c);\ \forall\, l \in \Omega^L,\ o,\ t,\ c,\ n = s(l) \tag{38}$$

$$Q_{lot}^c = A_l^c\cdot(\sqrt{2}(B_l + B_l^{sh}/2)u_{not}^c - B_l R_{lot}^c - G_l L_{lot}^c);\ \forall\, l \in \Omega^L,\ o,\ t,\ c,\ n = s(l) \tag{39}$$

$$-P_l^{max} \le P_{lot}^c \le P_l^{max}; \forall\, l \in \Omega^L,\, o,\, t,\, c \tag{40}$$

$$-Q_l^{max} \le Q_{lot}^c \le Q_l^{max}; \forall\, l \in \Omega^L,\, o,\, t,\, c \tag{41}$$

$$-\left(1-\sum_{\forall \tau \le t} x_{l\tau}\cdot A_l^c\right)\cdot M \le P_{lot}^c - \{\sqrt{2}G_l u_{not}^c - G_l R_{lot}^c + B_l L_{lot}^c\} \le \left(1-\sum_{\forall \tau \le t} x_{l\tau}\cdot A_l^c\right)\cdot M; \forall\, l \in \Omega^{L+},\, o,\, t,\, n = s(l),\, c \tag{42}$$

$$-\left(1-\sum_{\forall \tau \le t} x_{l\tau}\cdot A_l^c\right)\cdot M \le Q_{lot}^c - \{\sqrt{2}(B_l + \frac{B_l^{sh}}{2})u_{not}^c - B_l R_{lot}^c - G_l L_{lot}^c\} \le \left(1-\sum_{\forall \tau \le t} x_{l\tau}\cdot A_l^c\right)\cdot M; \forall\, l \in \Omega^{L+},\, o,\, t,\, n = s(l),\, c \tag{43}$$

$$-P_l^{max}\cdot \sum_{\forall \tau \le t} x_{l\tau}\cdot A_l^c \le P_{lot}^c \le P_l^{max}\cdot \sum_{\forall \tau \le t} x_{l\tau}\cdot A_l^c; \forall\, l \in \Omega^{L+},\, o,\, t,\, c \tag{44}$$

$$-Q_l^{max}\cdot \sum_{\forall \tau \le t} x_{l\tau}\cdot A_l^c \le Q_{lot}^c \le Q_l^{max}\cdot \sum_{\forall \tau \le t} x_{l\tau}\cdot A_l^c; \forall\, l \in \Omega^{L+},\, o,\, t,\, c \tag{45}$$

$$0 \le P_{got}^c \le P_g^{max}\cdot A_g^c; \forall\, g \in \Omega^G,\, o,\, t,\, c \tag{46}$$

$$0 \le P_{got}^c \le P_g^{max}\cdot \sum_{\forall \tau \le t} x_{g\tau}\cdot A_g^c; \forall\, g \in \Omega^{G+},\, o,\, t,\, c \tag{47}$$

$$0 \le Q_{got}^c \le Q_g^{max}\cdot A_g^c; \forall\, g \in \Omega^G,\, o,\, t,\, c \tag{48}$$

$$0 \le Q_{got}^c \le Q_g^{max}\cdot \sum_{\forall \tau \le t} x_{g\tau}\cdot A_g^c; \forall\, g \in \Omega^{G+},\, o,\, t,\, c \tag{49}$$

$$A_g^c\cdot(P_{got} - \Delta_g^{max}) \le P_{got}^c \le A_g^c\cdot(P_{got} + \Delta_g^{max}); \forall\, o,\, t,\, g,\, c \tag{50}$$

The formulated security-constrained dynamic G&TEP is an MINLP problem that is generally intractable for large-scale (even medium-scale) systems. Thus, a linearized version of the model is desired. The product of binary variables x_{lt}/x_{gt} and continuous variable Γ_{dot}^c in (34) is the only nonlinear term. We propose a big-M linearization method to obtain an MISOCP model for security-constrained dynamic G&TEP problem.

First, the nonlinear terms are replaced by an auxiliary variable γ_{dot}^c as shown in (51). Afterward, linear constraints (52)–(57), which restrict the auxiliary variable to get values equivalent to the values of the nonlinear term, must be added in the model. For existing transmission lines and generating units, the auxiliary variable must be equal to the expected energy not supplied during contingency (Γ_{dot}^c), as forced by (52) and (55). As imposed by (53), if the candidate transmission line is not planned to be built at the beginning of the planning period t and it was not built in previous periods, the auxiliary variable γ_{dot}^c is equal to zero. In this case, constraint (54) is inactive. On the other hand, if the candidate line is planned to be built at planning period t or it was built in advance, the auxiliary variable is equal to the expected energy not supplied during contingency (Γ_{dot}^c) as forced by (54). In this case, constraint (53) is inactive. Equations (56) and (57) impose the same logic for the candidate generating units.

$$\min_{\Delta,\Delta^c} \sum_{\forall t} \{a_{lt} \sum_{l\in\Omega^{L+}} \widetilde{I}_l\cdot x_{lt} + a_{gt} \sum_{g\in\Omega^{G+}} \widetilde{I}_g\cdot x_{gt} + \sum_{\forall o} \rho_o [\sum_{\forall g} C_g\cdot P_{got} + \sum_{\forall d} C_{dot}\cdot\Gamma_{dot} + \sum_{\forall c\in\{\Omega_c^L,\Omega_c^{L+}\}} \sum_{\forall d} C_{dot}^c\cdot\gamma_{dot}^{c,l} + \sum_{\forall c\in\{\Omega_c^G,\Omega_c^{G+}\}} \sum_{\forall d} C_{dot}^c\cdot\gamma_{dot}^{c,g}]\} \tag{51}$$

$$\gamma_{dot}^{c,l} = \Gamma_{dot}^c; \forall\, d,\, o,\, t,\, c \in \Omega_c^L \tag{52}$$

$$-\sum_{\forall \tau \le t} x_{l\tau}\cdot M \le \gamma_{dot}^{c,l} \le \sum_{\forall \tau \le t} x_{l\tau}\cdot M; \forall\, d,\, o,\, t,\, c \in \Omega_c^{L+} \tag{53}$$

$$-\left(1-\sum_{\forall \tau \le t} x_{l\tau}\right)\cdot M + \Gamma_{dot}^c \le \gamma_{dot}^{c,l} \le \left(1-\sum_{\forall \tau \le t} x_{l\tau}\right)\cdot M + \Gamma_{dot}^c; \forall\, d,\, o,\, t,\, c \in \Omega_c^{L+} \tag{54}$$

$$\gamma_{dot}^{c,g} = \Gamma_{dot}^c; \forall\, d,\, o,\, t,\, c \in \Omega_c^G \tag{55}$$

$$-\sum_{\forall \tau \le t} x_{g\tau}\cdot M \le \gamma_{dot}^{c,g} \le \sum_{\forall \tau \le t} x_{g\tau}\cdot M; \forall\, d,\, o,\, t,\, c \in \Omega_c^{G+} \tag{56}$$

$$-\left(1-\sum_{\forall \tau \le t} x_{g\tau}\right)\cdot M + \Gamma_{dot}^c \le \gamma_{dot}^{c,g} \le \left(1-\sum_{\forall \tau \le t} x_{g\tau}\right)\cdot M + \Gamma_{dot}^c; \forall\, d,\, o,\, t,\, c \in \Omega_c^{G+} \tag{57}$$

Finally, as an MISOCP model, the solution of the security-constrained dynamic G&TEP problem can be obtained by minimizing (51) subject to (3)–(12), (15)–(29), (33), (23)–(29) for each contingency $\boldsymbol{c}$, (33) for each contingency $\boldsymbol{c}$, (36)–(50), and (52)–(57).

3. Proposed Risk-Based dynamic G&TEP

The formulated MISOCP model can be solved by standard solvers [14]. However, one question should be answered: "what will be the value of load shedding penalty cost under a contingency (C_{dot}^c) in the objective function (51)?"

Different contingencies have different probabilities and consequences on the system. Depending on the system topology and characteristics, some contingencies might lead to further outages, and extremely, cascading failure [9]. Therefore, considering constant or identical values for penalty coefficients C_{dot}^c for all demand points is an oversimplification. We propose the concept of *risk* for each contingency to obtain a solution that prevents cascading failures in the planned system. The concept of risk is proposed to be incorporated into C_{dot}^c to cover the probability and also the propagating consequence of contingencies. Note, in the proposed risk-based dynamic G&TEP model, the penalty coefficients C_{dot}^c are variables rather than constant parameters as assumed in the existing literature.

3.1. Contingency probability

The probability of unscheduled outage of an individual component depends, mainly, on the component's failure rate and environmental conditions. Conventionally, the Markov chain model has been used for estimating the probability of a contingency [15]. In this paper, we assumed that the system has been observed for a long enough period, and therefore, historical data of outages are available. Using recorded historical data, a forced outage rate (FOR), λ, can be assigned to each component. For instance, if the number of unscheduled outages for a specific component during the past five periods are equal to $\{1, 2, 0, 3, 1\}$, then $\lambda = 1.4$. The advantage of using historical data of an operating component for estimating λ is that both component failure rate and environmental conditions are considered in the estimation. Concretely, by increasing the size of historical data, the estimated λ will be closer to its true value.

After estimating λ, the probability of having at least one outage during the next planning period can be obtained using the Poisson cumulative probability function (58), where x is the number of outages.

$$P(x, \lambda) = \sum_{i=1}^{x} \frac{e^{-\lambda}\cdot\lambda^i}{i!} \tag{58}$$

3.2. Propagating consequence of contingencies

To model how the consequence of each contingency is propagated over the system, two performance indices are introduced: MW performance index and voltage-reactive power performance index. To analyze contingency consequences using performance indices, the annual demand growth rate needs to be considered. The demand d for operating condition o in period t is obtained by (59), where P_{do1} is the demand at the first period.

$$P_{dot} = P_{do1}(1 + rate)^{t-1};\ \forall\ d,\ o,\ t \tag{59}$$

3.2.1. MW performance index

The proposed MW performance index represents the change of active power of transmission lines due to a line or generating unit outage. The MW performance index for operating condition o under contingency c is calculated by (60), where ΔP_{lot}^{c} is the change of power in line l due to contingency c, P_l^{max} is the maximum thermal capacity of line l, w_l is a desired weight coefficient, and m is a specified exponent (e.g., $m = 1$). The change in the active power of line l after the occurrence of contingency c can be either obtained from the recorded historical data or approximated using sensitivity factors of the system by (61) and (62), where $P_{lot}^{c}(0)$ and $P_{got}^{c}(0)$ are the pre-fault values of line flow and unit production, respectively. Line outage distribution factor (LODF) and shift factor (SF) are sensitivity factors that are calculated using the inverse admittance matrix of the system [16].

$$PI_{MW}(c,\ o,\ t) = \sum_{\forall l} \frac{w_l}{2m}\left(\frac{\Delta P_{lot}^{c}}{P_l^{max}}\right)^{2m};\ \forall\ c,\ o,\ t \tag{60}$$

$$\Delta P_{lot}^{c} \cong LODF_l^{c}\cdot P_{lot}^{c}(0);\ \forall\ l,\ t,\ c \in \{\Omega_c^{L},\ \Omega_c^{L+}\} \tag{61}$$

$$\Delta P_{lot}^{c} \cong SF_g^{c}\cdot P_{got}^{c}(0);\ \forall\ l,\ t,\ c \in \{\Omega_c^{G},\ \Omega_c^{G+}\} \tag{62}$$

3.2.2. Voltage-reactive power performance index

This performance index is proposed to model the effect of an outage on post-contingency voltage violation and reactive power deficiency of certain buses. Violation in voltage of a certain bus is, usually, because of the lack of enough reactive power transferred to that bus. This problem is more critical in weakly connected buses and after outages that might lead to a system islanding [17]. Hence, considering this performance index in the planning step is advantageous for voltage regulation. The voltage-reactive power performance index for operating condition o under contingency c is modeled by (63), where u_{not}^{c} is the post-contingency voltage magnitude at bus n, u_n^{rated} is the rated voltage magnitude at bus n, Δu_n^{lim} is the voltage deviation limit at bus n, Q_{got}^{c} is the reactive power produced by unit g after the occurrence of contingency c, and Q_g^{max} is the reactive power capacity of unit g. Post-contingency voltages and reactive power injected to buses can be either obtained from the recorded historical data or calculated from AC load flow analysis for each contingency considering the annual demand growth rate (see (59)). We assume that the historical data (e.g., obtained from PMUs) are available.

$$PI_{VQ}(c,\ o,\ t) = \sum_{\forall n} \frac{w_V}{2m}\left(\frac{|u_{not}^{c}| - |u_n^{rated}|}{\Delta u_n^{lim}}\right)^{2m} + \sum_{\forall g} \frac{w_Q}{2m}\left(\frac{Q_{got}^{c}}{Q_g^{max}}\right)^{2m};\ \forall\ c,\ o,\ t \tag{63}$$

3.3. Risk indices

Having the performance indices for each operating condition, the proposed risk index is computed by (64), which includes both the probability and consequence of each contingency. The proposed post-contingency load shedding penalty cost is defined based on the calculated risk indices and C_{dot} as in (65). Note that C_{dot} (which is called *the value of lost load* in the literature) depends on the importance of forecasted demand and is a fixed value for each demand d in operating condition o [18].

$$RI(c,\ o,\ t) = P(x \geq 1,\ \lambda)\cdot(PI_{MW}(c,\ o,\ t) + PI_{VQ}(c,\ o,\ t));\ \forall\ c,\ o,\ t \tag{64}$$

$$C_{dot}^{c} = RI(c,\ o,\ t) \times C_{dot};\ \forall\ c,\ d,\ o \tag{65}$$

3.4. Risk-based dynamic G&TEP model

Consider the objective function (51). Using the auxiliary variables $\omega_{dot}^{c,l}$ and $\omega_{dot}^{c,g}$, (66) is equivalent to (51) if (67) and (68) are valid.

$$\min_{\Delta,\Delta^c} \sum_{\forall t} \Big\{ a_{lt} \sum_{l\in\Omega^{L+}} \widetilde{I}_l\cdot x_{lt} + a_{gt} \sum_{g\in\Omega^{G+}} \widetilde{I}_g\cdot x_{gt} + \sum_{\forall o} \rho_o \Big[\sum_{\forall g} C_g\cdot P_{got} + \sum_{\forall d} C_{dot}\cdot\Gamma_{dot} + \sum_{\forall c\in\{\Omega_c^{L},\Omega_c^{L+}\}} \sum_{\forall d} \omega_{dot}^{c,l} + \sum_{\forall c\in\{\Omega_c^{G},\Omega_c^{G+}\}} \sum_{\forall d} \omega_{dot}^{c,g} \Big] \Big\} \tag{66}$$

$$\omega_{dot}^{c,l} = C_{dot}^{c}\cdot\gamma_{dot}^{c,l};\ \forall\ d,\ o,\ t,\ c \in \{\Omega_c^{L},\ \Omega_c^{L+}\} \tag{67}$$

$$\omega_{dot}^{c,g} = C_{dot}^{c}\cdot\gamma_{dot}^{c,g};\ \forall\ d,\ o,\ t,\ c \in \{\Omega_c^{G},\ \Omega_c^{G+}\} \tag{68}$$

However, since C_{dot}^{c} is a variable in the proposed risk-based model, equality constraints (67) and (68) include bilinear terms. We apply McCormick relaxation to linearize the bilinear terms [19]. Having equality constraints (67) and (68), corresponding McCormick envelops are presented in (69)–(76). McCormick underestimators and overestimators for (67) are given by (69)–(70) and (71)–(72), respectively. A similar sequence is conformed in (73)–(76) to linearize (68). McCormick envelops and other relaxation techniques do not guarantee the satisfaction of equality constraints (67) and (68). However, they can provide a near-optimal solution if the relaxation is tight enough. Applying approximation techniques (e.g., linearization) and relaxation techniques (e.g., McCormick envelops) are a common practice, which is widely reported in the literature, to relieve the intractability of MINLP problems.

$$\omega_{dot}^{c,l} \geq 0;\ \forall\ d,\ o,\ t,\ c \in \{\Omega_c^{L},\ \Omega_c^{L+}\} \tag{69}$$

$$\omega_{dot}^{c,l} \geq C_{dot}\cdot\gamma_{dot}^{c,l} + C_{dot}^{c}\cdot P_{dot} - C_{dot}\cdot P_{dot};\ \forall\ d,\ o,\ t,\ c \in \{\Omega_c^{L},\ \Omega_c^{L+}\} \tag{70}$$

$$\omega_{dot}^{c,l} \leq C_{dot}\cdot\gamma_{dot}^{c,l};\ \forall\ d,\ o,\ t,\ c \in \{\Omega_c^{L},\ \Omega_c^{L+}\} \tag{71}$$

$$\omega_{dot}^{c,l} \leq C_{dot}^{c}\cdot P_{dot};\ \forall\ d,\ o,\ t,\ c \in \{\Omega_c^{L},\ \Omega_c^{L+}\} \tag{72}$$

$$\omega_{dot}^{c,g} \geq 0;\ \forall\ d,\ o,\ t,\ c \in \{\Omega_c^{G},\ \Omega_c^{G+}\} \tag{73}$$

$$\omega_{dot}^{c,g} \geq C_{dot}\cdot\gamma_{dot}^{c,g} + C_{dot}^{c}\cdot P_{dot} - C_{dot}\cdot P_{dot};\ \forall\ d,\ o,\ t,\ c \in \{\Omega_c^{G},\ \Omega_c^{G+}\} \tag{74}$$

$$\omega_{dot}^{c,g} \leq C_{dot}\cdot\gamma_{dot}^{c,g};\ \forall\ d,\ o,\ t,\ c \in \{\Omega_c^{G},\ \Omega_c^{G+}\} \tag{75}$$

$$\omega_{dot}^{c,g} \leq C_{dot}^{c}\cdot P_{dot};\ \forall\ d,\ o,\ t,\ c \in \{\Omega_c^{G},\ \Omega_c^{G+}\} \tag{76}$$

Finally, the proposed risk-based dynamic G&TEP model is to minimize (66) subject to (3)–(12), (15)–(29), (33), (23)–(29) for each contingency c, (33) for each contingency c, (36)–(50), (52)–(57), (59)–(65), and (69)–(76).

4. Case study

The proposed risk-based dynamic G&TEP model is tested on the IEEE RTS 24-bus system. Simulations are carried out using GAMS and CPLEX 12.7 solver with default options [20]. The optimality gap of the solver is set to zero for all cases (optcr = 0). A personal computer with an Intel(R) Xeon(R) CPU @2.6 GHz, including eight cores and 16 GB of RAM, is used. A one-line diagram of the system is shown in Fig. 1. The system consists of 18 existing generating units, 17 loads, and 34 existing transmission lines. The system parameters are given in [21], and the branch data for the SOCP model is attained from [22]. Annual

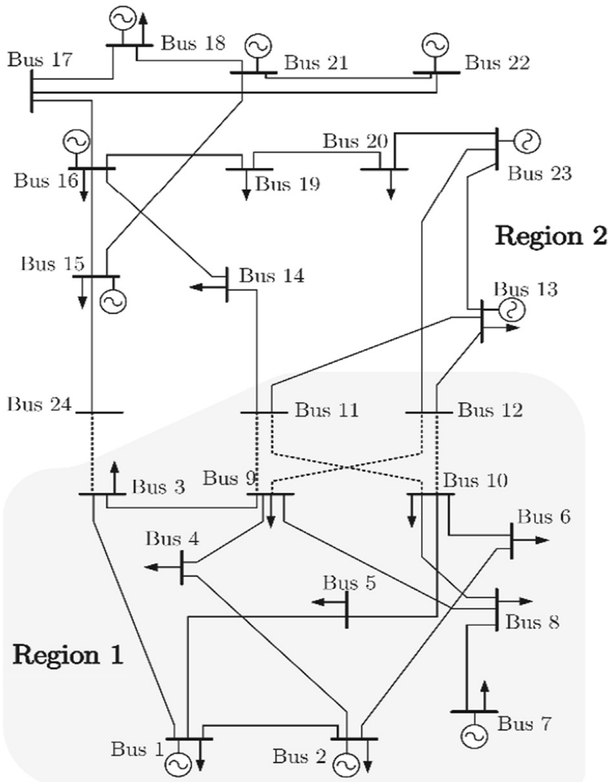

Fig. 1. One-line diagram of the IEEE 24-bus system [21].

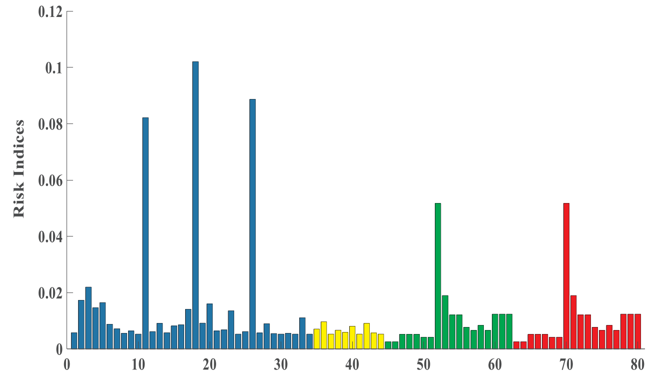

Fig. 2. Values of 80 risk indices of the IEEE 24-bus system (case 3).

planning periods for a planning horizon of five years is considered. The peak load is assumed to be 800 MW for the first year with an annual increase rate of 1%. Four operating conditions with the load factors of {0.5, 0.65, 0.9, 1} and weights (hours per year) of {1510, 2800, 2120, 2330} are assumed. Ten candidate lines and 18 candidate units are considered. Table 1 includes candidate lines parameters. Generation capacity, operation cost, and location of the candidate units are assumed to be the same as the existing units. The investment cost of each candidate unit is assumed to be 50 Million dollars. The amortization rate for both candidate transmission lines and generating units is 20% (i.e., $\alpha_{lt} = \alpha_{gt} = 0.2$).

For the studied system, a maximum number of 80 individual contingency is considered, which are outages of 34 existing lines, ten candidate lines, 18 existing units, and 18 candidate units. Four cases are studied:

Case 1: The conventional dynamic G&TEP problem, which is modeled in Section 2.1, is considered in this case. That is, load shedding penalty cost under a contingency (C^c_{dot}) is set to zero, and all contingency constraints are eliminated. The objective function is 478.75 Million dollars. Three new lines and six new generating units are planned to be installed.

Case 2: The security-constrained dynamic G&TEP problem, which is modeled in Section 2.2, is considered. Contingencies are assumed to have the same probability and consequence. All risk indices are set to one over the number of contingencies (i.e., $C^c_{dot} = (\frac{1}{180}) \times C_{dot}$). The objective function is 483.88 Million dollars. Eight new lines and six new generating units are planned to be installed. The cost increment observed in this case as compared to case 1 is the reliability cost, which must be paid to keep the system reliable even after the occurrence of a contingency.

Case 3: The proposed risk-based dynamic G&TEP problem, which is modeled in Section 3.4, is studied. The objective function is 481.80 Million dollars. Six new lines and six new generating units are planned to be installed. Fig. 2 depicts the calculated values of 80 risk indices each of which corresponds to an outage. Five critical contingencies exist, which are associated with the outage of existing lines 7–8, 11–13, 15–24, and the outage of existing and candidate units located on bus 13. This means that the load shedding penalty cost under a contingency (C^c_{dot}) is dominant for these five outages.

Case 4: The proposed risk-based dynamic G&TEP problem is studied. Fifty-two operation conditions are considered. Load factors are randomly generated and normalized in a way that their summation equals to one. Similar weights (i.e., $\frac{1}{52}$) is considered for all operating conditions. The model converges in 812.6 min, which is a reasonable runtime for a long-term planning problem. Six new lines and six new generating units are planned to be installed. The objective function is \$482.36 Million.

A comparison between the results of the four cases is presented in Table 2. Concretely, because of $N-1$ security criteria modeling, the objective function calculated for cases 2 and 3 is higher than that of case 1. According to the standards, this additional cost is necessary and must be paid to keep the reliability of the planned system within an acceptable level [4]. Comparing with case 2, the proposed risk-based dynamic G&TEP considered in case 3 converges to a more desired solution. The objective function and generation cost of units calculated in

Table 1
Candidate lines' parameters for the IEEE RTS 24-bus system.

Line No.	From bus	To bus	G_l (pu)	B_l (pu)	B_l^{sh} (pu)	Capacity (MW)	Investment cost (M$)
1	3	14	0.5	10	0.03	100	0.7
2	9	15	0.5	10	0.03	100	0.8
3	9	20	0.5	10	0.03	100	0.1
4	1	18	0.5	10	0.03	100	1.2
5	1	22	0.5	10	0.03	100	1.3
6	2	23	0.5	10	0.03	100	1.1
7	6	19	0.5	10	0.03	100	0.9
8	7	8	0.5	10	0.03	100	0.5
9	7	1	0.5	10	0.03	100	0.4
10	7	2	0.5	10	0.03	100	0.6

Table 2
Comparison between results of different cases.

Case	Obj. function [M$]	Investment cost for candidate lines [M$]	Installed candidate lines	Investment cost for units [M$]	Installed units	Generation cost of units [M$]	Cost of load shedding in normal operation [M$]	Cost of post-contingency load shedding [M$]	CPU time [Minutes]
1	478.75	T1 = 0.38	T1 = 1, 2, 9	T1 = 60	T1 = 1–5, 7	T1 = 70.91 T2 = 76.74 T3 = 82.93 T4 = 89.92 T5 = 97.87	0	0	4.1
2	483.88	T1 = 0.24 T2 = 0.48 T3 = 0.32 T4 = 0.16 T5 = 0.08	T1 = 4 T2 = 5, 8, 10 T3 = 1, 7 T4 = 2 T5 = 9	T1 = 60	T1 = 1–5, 7	T1 = 70.97 T2 = 76.77 T3 = 83.26 T4 = 90.38 T5 = 98.63	0	T1 = 0 T2 = 0.19 T3 = 0.08 T4 = 0.67 T5 = 1.65	22.5
3	481.80	T1 = 0.34 T2 = 0.14 T3 = 0 T4 = 0.12 T5 = 0.26	T1 = 2, 8, 9 T2 = 1 T4 = 10 T5 = 5	T1 = 60	T1 = 1–5, 7	T1 = 71.13 T2 = 76.74 T3 = 83.09 T4 = 89.92 T5 = 98.58	0	T1 = 0 T2 = 0 T3 = 0 T4 = 0.36 T5= 1.12	23.4
4	482.36	T1 = 0.34 T2 = 0.14 T3 = 0 T4 = 0.12 T5 = 0.26	T1 = 2, 8, 9 T2 = 1 T4 = 10 T5 = 5	T1 = 60	T1 = 1–5, 7	T1 = 71.15 T2 = 76.73 T3 = 83.11 T4 = 89.99 T5 = 98.68	0	T1 = 0 T2 = 0 T3 = 0 T4 = 0.41 T5 = 1.33	812.6

case 3 are less than those obtained in case 2. Furthermore, the proposed method of case 3 reduces the cost of post-contingency load shedding by installing fewer lines (six new lines rather than eight lines suggested by case 2).

Generally, due to nonconvex nature, it is difficult to interpret the solution of mixed-integer programming problems. However, some intuitions can be expressed as follows:

- One example of a high-risk contingency is the outage of existing line 7–8 that causes islanding of bus 7 (see Fig. 1). It can also be detected by the high-risk index obtained for this contingency (contingency number 11 in Fig. 2). Consequently, installation of candidate line 8, which is a new path between buses 7 and 8, is an appropriate decision to avoid this high-risk contingency. Besides, by installing candidate line 8, the cost of post-contingency load shedding can be reduced considerably. This decision is made for the first year by the proposed risk-based model, while the security-constrained model addressed in case 2 suggests this decision for the second year (see Table 2). This illustrates the superiority of the proposed risk index-based model.
- Two of the other detected high-risk contingencies are associated with the outage of existing lines 11–13 and 15–24 (contingencies number 18 and 26 in Fig. 2). This is because of a weak connection between region one and region two (note that the IEEE 24-bus test system is modified in [21] to make it suitable for network expansion studies). All existing lines have a capacity of 100 MW, except for tie lines (distinguished by dashed lines in Fig. 1) that have a capacity of 20 MW. Therefore, any new line making a new connection between regions one and two is desired. For this purpose, candidate line two can connect buses nine and bus 15. The proposed risk-based model suggests that candidate line two should be installed in the first year, while the security-constrained model addressed in case 2 suggests this installation for the fourth year (see Table 2). This demonstrates the superiority of the proposed risk index-based model.

Table 3
Model statistics of different cases.

Case	Number of constraints	Number of continuous variables	Number of binary variables
1	2499	2466	140
2	189,704	196,066	140
3	272,664	250,466	140
4	7,085,779	6,511,491	140

Note that in Table 2, the investment cost for candidate lines is the planning decision that must be paid. The generation cost of units will be paid if the forecast demand is realized in the real-time operation, and the penalty cost of post-contingency load shedding is just a measure representing the reliability and robustness of the planned system. Table 3 presents model statistics for all cases.

5. Conclusion

A risk-based dynamic G&TEP model with respect to the propagating effect of each contingency on the system is proposed in this paper. The proposed model takes advantage of risk indices to consider the non-identical probability and consequence of individual contingencies. To keep the practicality of the proposed method, an SOCP model is applied for power flow representation, and the problem is modeled in a dynamic time frame. The McCormick relaxation was tailored to make the model linear. The numerical analysis of the proposed model on the IEEE RTS 24-bus system illustrates the advantages of distinguishing high-risk contingencies and reducing the post-contingency load shedding cost. That is, using the proposed approach, the planned system is more robust against contingencies, especially high-risk outages and those that result in cascading failures. Therefore, it can be concluded that using the proposed risk-based G&TEP model, the investment budget for keeping power system reliability during an expansion planning will be spent more wisely.

Declaration of Competing Interest

Not applicable.

Acknowledgement

This work was supported partly by the Louisiana Board of Regents grant LEQSF 2016-19-RD-A-10 and partly by the National Science Foundation grant ECCS-1711850.

Appendix A. Nomenclature

A. Indices and Sets:	
c	Index for contingencies.
d	Index for demand.
g	Index for generating units.
l	Index for transmission lines.
n	Index for buses.
o	Index for operating conditions.
t	Time periods.
$r(l)$	Receiving-end node of transmission line l.
$s(l)$	Sending-end node of transmission line l.
Ω^L	Set of all existing transmission lines.
Ω^{L+}	Set of all candidate transmission lines.
Ω^G	Set of all existing generating units.
Ω^{G+}	Set of all candidate generating units
Ω_c^L	Set of all contingencies in existing lines.
Ω_c^{L+}	Set of all contingencies in candidate lines.
Ω_c^G	Set of all contingencies in existing units.
Ω_c^{G+}	Set of all contingencies in candidate units.
B. Parameters:	
A_g^C, A_l^C	Parameter that is equal to 0 if unit g/line l is unavailable under contingency c, and 1 otherwise.
B_l	Series susceptance in π-model of transmission line l.
B_l^{sh}	Shunt susceptance in π-model of transmission line l.
C_{dot}	Load-shedding cost of demand d.
C_{dot}^c	Load-shedding cost of demand d in time period t during contingency c.
C_g	Production cost of generating unit g.
P_l^{max}/Q_l^{max}	Active/reactive capacity of transmission line l.
G_l	Series conductance in π-model of transmission line l.
$\tilde{I}_l$	Investment cost of candidate transmission line l.
$\tilde{I}_g$	Investment cost of candidate generating unit g.
$\tilde{I}_{lt}^{max}$	Investment budget for building new transmission lines in time period t.
$\tilde{I}_{gt}^{max}$	Investment budget for building new generating units in time period t.
M	Large enough numbers, called big-M.
P_{dot}	Value of demand d in operating condition o of time period t.
P_g^{max}/Q_g^{max}	Maximum active/reactive capacity of unit g.
α_l, α_g	Amortization rate for investment cost of transmission line l/generating unit g.
$\alpha_{\rm d}$	A positive constant.
ρ_o	Weight of operating condition o [hours].
PI_{MW}	Megawatt performance index.
PI_{VQ}	Voltage-reactive power performance index.
Δ_g^{max}	Maximum adjustment capability of unit g.
C. Variables:	
x_{lt}/x_{gt}	Binary decision variable to indicate whether candidate line l/generating unit g is constructed in time period t.
P_{got}/Q_{got}	Active/reactive power generation of unit g in operating condition o of time period$t$
P_{got}^c/Q_{got}^c	Active/reactive power generation of unit g in operating condition o of time period t during contingency c.
P_{lot}/Q_{lot}	Active/reactive power flow through line l in operating condition o of time period t.
P_{lot}^c/Q_{lot}^c	Active/reactive power flow through line l in operating condition o of time period t during contingency c.
u_{not}	Auxilary variable of voltage magnitude in conic model.
R_{lot}	Auxiliary variable for conic AC power flow model.
L_{lot}	Auxiliary variable for conic AC power flow model.
V_{not}	Voltage magnitude at node n in operating condition o of time period t.
θ_{not}	Voltage angle at node n in operating condition o of time period t.
$\Gamma_{dot}/\Gamma_{dot}^c$	Expected energy not supplied for demand d in operating condition o of time period t during normal operation/contingency c.
γ_{dot}^c	An auxiliary variable defined for linearization.
$\omega_{dot}^{c,l}/\omega_{dot}^{c,g}$	Auxiliary variables defined for McCormick envelops.

Appendix B. Supplementary material

Supplementary data to this article can be found online at https://doi.org/10.1016/j.ijepes.2019.105762.

References

[1] Mehrtash M. Optimal and efficient decision-making for power system expansion planning. ECE: Louisiana State University; 2019.
[2] Conejo AJ, Baringo L, Kazempour SJ, Siddiqui AS. Investment in electricity generation and transmission. Springer International Publishing; 2016.
[3] Rashidaee SA, Amraee T, Fotuhi-Firuzabad M. A linear model for dynamic generation expansion planning considering loss of load probability. IEEE Trans Power Syst 2018.
[4] NERC. Transmission System Adequacy and Security [Online]. Available: http://www.nerc.com.
[5] Majidi-Qadikolai M, Baldick R. Integration of N-1 contingency analysis with systematic transmission capacity expansion planning: ERCOT case study. IEEE Trans Power Syst 2016;31(3):2234–45.
[6] Majidi-Qadikolai M, Baldick R. Stochastic transmission capacity expansion planning with special scenario selection for integrating N-1 contingency analysis. IEEE Trans

Power Syst 2016;31(6):4901–12.
[7] Choi J, Tran T, El-Keib A, Thomas R, Oh H, Billinton R. A method for transmission system expansion planning considering probabilistic reliability criteria. IEEE Trans Power Syst 2005;20(3):1606–15.
[8] Aghaei J, Amjady N, Baharvandi A, Akbari M-A. Generation and transmission expansion planning: MILP–based probabilistic model. IEEE Trans Power Syst 2014;29(4):1592–601.
[9] Armaghani S, Naghshbandy AH, Shahrtash SM. A novel multi-stage adaptive transmission network expansion planning to countermeasure cascading failure occurrence. Int J Electr Power Energy Syst 2020;115:105415.
[10] Mehrtash M, Mohammadi A, Barati M, Kargarian A. Security-Constrained transmission expansion planning with risk index of N-1 security obtained from PMU Data. 2018 IEEE Power & Energy Society General Meeting (PESGM). IEEE; 2018. p. 1–5.
[11] Jabr RA. Optimization of AC transmission system planning. IEEE Trans Power Syst 2013;28(3):2779–87.
[12] Haghighat H, Zeng B. Bilevel conic transmission expansion planning. IEEE Trans Power Syst 2018;33(4):4640–2.
[13] Mehrtash M, Kargarian A, Mohammadi A. Distributed optimisation-based collaborative security-constrained transmission expansion planning for multi-regional systems. IET Gener Transm Distrib 2019;13(13):2819–27.
[14] Drewes S, Ulbrich S. Mixed integer second order cone programming. Verlag Dr. Hut; 2009.
[15] Xiao F, McCalley JD, Ou Y, Adams J, Myers S. Contingency probability estimation using weather and geographical data for on-line security assessment. PMAPS 2006. International Conference on Probabilistic Methods Applied to Power Systems, 2006. IEEE; 2006. p. 1–7.
[16] Wood AJ, Wollenberg BF. Power generation, operation, and control. John Wiley & Sons; 2012.
[17] Kargarian A, Raoofat M, Mohammadi M. Reactive power provision in electricity markets considering voltage stability and transmission congestion. Electr Power Compon Syst 2011;39(12):1212–26.
[18] Schröder T, Kuckshinrichs W. Value of lost load: an efficient economic indicator for power supply security? A literature review. Front Energy Res 2015;3:55.
[19] Tsoukalas A, Mitsos A. Multivariate mccormick relaxations. J Global Optim 2014;59(2–3):633–62.
[20] IBM ILOG CPLEX Optimizer software. Available: https://www-01.ibm.com/software/commerce/optimization/cplex-optimizer/.
[21] Ruiz C, Conejo AJ. Robust transmission expansion planning. Eur J Oper Res 2015;242(2):390–401.
[22] Rider M, Garcia A, Romero R. Power system transmission network expansion planning using AC model. IET Gener Transm Distrib 2007;1(5):731–42.